HAIT Journal of Science and Engineering A, Volume 5, Issues 1-2, pp. 93-111
Copyright © 2008 Holon Institute of Technology

From spin and orbital SU(4) to spin SU(2) Kondo effect in double quantum dot

Alexander L. Chudnovskiy[1], Frank Hellmuth[1],
and Victor Kagalovsky[2,*]

[1] *Institut für Theoretische Physik, Universität Hamburg, Jungiusstr. 9, 20355 Hamburg, Germany*
[2] *Sami Shamoon College of Engineering, Beer-Sheva, 84100, Israel*
Corresponding author: victork@sce.ac.il

Received 21 September 2007

Abstract

We consider spin and orbital Kondo effect in a parallel arrangement of two strongly electrostatically coupled quantum dots. Increasing the exchange of electrons between the dots through the attached leads induces a smooth crossover between $SU(4)$ spin- and orbital Kondo effect and $SU(2)$ spin Kondo effect. Being the same for the $SU(4)$ and $SU(2)$ symmetry points, the Kondo temperature drops slightly in the intermediate regime. Experimentally, two kinds of Kondo effect can be discriminated by the sensitivity to the suppression of the spin Kondo effect by Zeeman field. The dependence of the Kondo temperature and of the differential conductance on the strength of electronic exchange through the leads and Zeeman field is analyzed in detail.

PACS: 73.23.-b, 73.63.Kv, 72.15.Qm

1 Introduction

Kondo effect in quantum dot devices remains a subject of active theoretical and experimental investigations since its first observation [1]. The observation of the Kondo effect with orbitally degenerate levels provided the demonstration of a strong influence of the orbital structure of the states in

the dot and attached leads on the Kondo effect [2]. Further exploration of the interplay between spin and orbital degrees of freedom in the Kondo effect became possible in experiments with double quantum dot systems. If the two dots are strongly electrostatically coupled [3, 4], then there are regions in the charging diagram of the double dot device, where there is no energy cost to transfer an electron between the two dots. In that regions, the two ground states of the double dot system with occupations of the two dots $(N_1 - 1, N_2 + 1)$ and (N_1, N_2) are degenerate. Those ground states span a two-dimensional Hilbert space of the representation of the $SU(2)$ group, hence a spin-like degree of freedom called pseudospin can be assigned to them. Quite analogously to and to a large extent independently of the well-known spin Kondo effect, the orbital fluctuations in transport through the double quantum dot result in the development of the orbital, or pseudospin Kondo effect. Furthermore, at special values of Kondo couplings, the combined spin and pseudospin Kondo Hamiltonian possesses a $SU(4)$ symmetry with respect to rotations in spin-pseudospin space. In that regime, the $SU(4)$ Kondo effect with greatly enhanced Kondo temperature has been predicted theoretically [5, 6]. Another realization of the $SU(4)$ Kondo effect has been predicted theoretically for a system of a small quantum dot and a large grain. The signature of the $SU(4)$ Kondo effect in that system is a complete smearing of the Coulomb blockade oscillations in the grain [7]. Recently, spin and orbital $SU(4)$ Kondo effect has been observed experimentally in carbon nanotubes [8].

The existence of the pseudospin Kondo effect crucially relies on the coupling of each localized orbital state to its own reservoir of delocalized electrons. In the case of the double quantum dot, the reservoirs are formed by the electron states in the attached leads. The separation of the reservoirs allows to define a pseudospin for the electrons in the leads in a natural way. For two sequentially coupled quantum dots [5], or for a double dot in the Aharonov-Bohm configuration [9] such a separation is given by geometry. In contrast, the realistic experimental geometry for two dots coupled *in parallel* to the leads does not introduce a separate reservoir for each dot *a priori* [3].

In this paper, we investigate the possibility and properties of spin and pseudospin Kondo effect in a double dot embedded in a parallel circuit with the attached leads if there is no separate electron reservoirs for each quantum dot. The separation between the two electronic reservoirs is characterized by the asymmetry of amplitudes of each electronic mode to tunnel from the reservoir into one or into the other dot. We introduce a measure of mixing between the two reservoirs, which reflects the structure of tunnel matrix elements. In the limit of completely symmetric tunneling from each mode

to both quantum dots, the Kondo effect in the orbital sector is suppressed. At the same time, all modes of both reservoirs couple to a single electron state given by a symmetric combination of the states localized in each dot. This results in the doubling of the density of states in the reservoir for the spin Kondo effect. At the end, the Kondo temperatures for the two symmetry points, the $SU(4)$ one and the $SU(2)$ one, are equal [6, 9, 10, 11]. We find however that the Kondo temperature gets slightly suppressed in the intermediate regime between the two symmetry points (see inset in Fig. 2). The change in symmetry of the Kondo effect can be detected experimentally by applying an external Zeeman magnetic field. To exclude the effect of magnetic field on the orbital electron motion [9], the magnetic field should be applied in the plane of the double dot device. An external Zeeman field suppresses the Kondo effect in the spin sector. Therefore, whereas the $SU(2)$ Kondo effect is completely suppressed by the Zeemann field, the combined spin-pseudospin $SU(4)$ Kondo effect is only reduced to the $SU(2)$ Kondo effect in the pseudospin sector.

The rest of the paper is organized as follows: the theoretical model is introduced in Section 2. In Section 3 the renormalization group (poor man scaling) treatment is introduced. The results for the Kondo temperature as a function of mixing between the reservoirs and of a Zeeman magnetic field in the whole range between the $SU(4)$ and $SU(2)$ regimes are discussed. This part is an extension of the previous work of one of the authors [12]. The results on the conductance of the double quantum dot are presented in Section 4. Our findings are summarized in Section 5.

2 The model of double quantum dot

We consider a device consisting of two single-level quantum dots coupled in parallel to external Fermi liquid leads. The Hamiltonian represents a sum of the following terms: the Hamiltonian of isolated quantum dots including the interdot interaction, the Hamiltonian of Fermi liquid reservoirs, and the tunneling between the reservoirs and the dots

$$H = H_{QD} + \sum_{\nu=r,l} H_{\nu}^{\mathrm{res}} + H^{t}. \tag{1}$$

The Hamiltonian of isolated quantum dots reads

$$H_{QD} = \sum_{i=1,2} \left[\sum_{\sigma=\uparrow\downarrow} E_i \hat{n}_{i\sigma} + U \hat{n}_{i\uparrow} \hat{n}_{i\downarrow} \right] + U_{12} \hat{n}_1 \hat{n}_2, \tag{2}$$

where the following notations are introduced: $\hat{n}_{i\sigma} = \hat{c}^{\dagger}_{i\sigma}\hat{c}_{i\sigma}$ – the number of electrons in the dot i with spin-projection σ, $\hat{c}_{i\sigma}$ is an annihilation operator of an electron in dot i with spin projection σ. We focus on the $SU(4)$ Kondo regime that is achieved at $E_1 = E_2 = E$, $U_{12} = U$. The low energy sector of the model consists of states with a total of one electron in the double dot. Their energy in the isolated dots equals E (< 0). The corresponding ket-vectors are denoted as $|\sigma, 0\rangle$ and $|0, \sigma\rangle$, where $\sigma =\uparrow$ or $\downarrow$ refers to the z-projection of spin, and 0 denotes the unoccupied dot. Single particle tunneling transforms the low energy states into the empty state $|0, 0\rangle$ (energy 0) or into states with a total of two electrons (energy $E + U$ (> 0)), which are $|\uparrow\downarrow, 0\rangle$, $|0, \uparrow\downarrow\rangle$, $|\sigma_1, \sigma_2\rangle$. The excited states with a total of more than two electrons in the double dot do not couple to the low-energy sector in the second order in tunneling. They are omitted from consideration. The tunneling Hamiltonian is given by

$$H^t = \sum_{i=1,2} \sum_{r=s,d} \sum_{k\sigma} t^r_{ik} \hat{a}^{\dagger}_{rk\sigma} \hat{c}_{i\sigma} + h.c., \tag{3}$$

where $\hat{a}_{rk\sigma}$ is the annihilation operator of a fermion in the reservoir r with the wave vector k and z-projection of spin $\sigma =\uparrow, \downarrow$. We do not consider the effect of a perpendicular magnetic field throughout this work, then the tunnel matrix elements can be chosen real. To elucidate the appearance of the pseudospin in a general case, when each electronic mode has nonvanishing tunneling amplitudes to both quantum dots, let us define the tunneling angle η^r_k for each mode in the given reservoir by the following relations:

$$\cos(\eta^r_k) = \frac{t^r_{1k}}{t^r_k}, \tag{4}$$

$$\sin(\eta^r_k) = \frac{t^r_{2k}}{t^r_k}, \tag{5}$$

where $t^r_k = \sqrt{\left(t^r_{1k}\right)^2 + \left(t^r_{2k}\right)^2}$. In what follows we consider the case of symmetric couplings to both reservoirs, $\eta^s_k = \eta^d_k$ and omit the index of the reservoir by the tunneling angle. Furthermore, we introduce formally bi-spinor notations for the operators in the fermionic reservoir and in the double dot

$$\hat{\Psi}_{rk} = \left(\cos\eta^r_k, \sin\eta^r_k\right)^T \otimes \left(\hat{a}_{rk\uparrow}, \hat{a}_{rk\downarrow}\right)^T, \tag{6}$$

$$\hat{\Phi} = \left(\hat{c}_{1\uparrow}, \hat{c}_{1\downarrow}, \hat{c}_{2\uparrow}, \hat{c}_{2\downarrow}\right)^T. \tag{7}$$

In (6) the upper signs in the exponent relate to $r = s$ and the lower ones to $r = d$. Using the notations above, we rewrite the tunneling Hamiltonian in

the form

$$H^t = \sum_k t_k \left(\frac{t_k^s}{t_k} \hat{\Psi}^\dagger_{sk} + \frac{t_k^d}{t_k} \hat{\Psi}^\dagger_{dk} \right) \hat{\Phi} + h.c., \tag{8}$$

where $t_k = \sqrt{(t_k^s)^2 + (t_k^d)^2}$. One can see from (8) that for each k it is only the mode

$$\hat{\Psi}_k = \frac{t_k^s}{t_k} \hat{\Psi}_{sk} + \frac{t_k^d}{t_k} \hat{\Psi}_{dk} \tag{9}$$

that couples to the double dot [13]. Performing the Schriefer-Wolff transformation for Hamiltonian (1), we derive the effective Kondo Hamiltonian describing the dynamics of the low-energy sector of the model that can be written as

$$H_K = \sum_{\mu,\nu=0}^{3} \sum_{k,k'} J_{\mu\nu}^{kk'} \hat{\Phi}^\dagger \left(\hat{\tau}^\mu \otimes \hat{\tau}^\nu \right) \hat{\Phi} \hat{\Psi}^\dagger_k \left(\hat{\sigma}^\mu \otimes \hat{\sigma}^\nu \right) \hat{\Psi}_{k'} + H_{\rm res}. \tag{10}$$

Here $\hat{\Phi}^\dagger \left(\hat{\tau}^\mu \otimes \hat{\tau}^\nu \right) \hat{\Phi}$ and $\hat{\Psi}^\dagger_k \left(\hat{\sigma}^\mu \otimes \hat{\sigma}^\nu \right) \hat{\Psi}_k$ represent the "hyperspins" in the pseudospin-spin $SU(4)$ space for the double dot and fermionic reservoir respectively, $\hat{\tau}^\mu$ and $\hat{\sigma}^\mu$ denote the corresponding Pauli matrices. For the $SU(4)$ symmetry point, the Kondo couplings equal $J_{\mu\nu}^{kk'} = t_k t_{k'} \left(\frac{1}{E+U} - \frac{1}{E} \right)$ for all $\mu, \nu = \overline{0,3}$ except $\mu = \nu = 0$. Note the principal difference between the hyperspins in the quantum dot and in the reservoir. Whereas the operator $\hat{\Phi}$ incorporates four dynamical degrees of freedom, the operator $\hat{\Psi}_k$ does only two, $\hat{a}_{k\uparrow}$ and $\hat{a}_{k\downarrow}$. The angle η_k is not dynamical. Yet this angle can fluctuate with wave vector k. The magnitude of those fluctuations determines whether the pseudospin in reservoirs is promoted to a dynamical degree of freedom. For example, if the reservoirs for two quantum dots are strictly separated, the angle η_k assumes two possible values 0 and $\pi/2$, which results in strong fluctuations of η_k with k, and eventually leads to the pseudospin Kondo effect. In contrast, if there is only a single common reservoir for both dots, then the tunneling amplitudes to both dots are equal $t_{1k} = t_{2k}$ $\forall k$. In that case, the angle η_k is frozen at the value $\pi/4$ for any k, and the orbital Kondo effect is suppressed.

3 Kondo temperature

In what follows we present results on the dependence of Kondo temperature on the mixing between the reservoirs b_1 obtained by the renormalization group (or poor man scaling) treatment of the Hamiltonian (10). We assume

the values t_k^r that reflect the total tunneling probability from a given mode of a reservoir into the double dot to be k-independent for energies close to the Fermi level of the reservoirs, $t_k^r = t^r$. Then the Kondo coupling constants $J_{\mu\nu}^{kk'}$ become independent of the wave vectors, $J_{\mu\nu}^{kk'} = J_{\mu\nu}$. The one loop renormalization of the Kondo couplings $J_{\mu\nu}$ is given by the diagram in Fig. 1 and the diagrams obtained by change of direction of arrows for solid or dashed lines.

Figure 1: One loop renormalization of Kondo coupling. Solid line: the propagator of electrons in the reservoir $\hat{G}(\omega, k)$. Dashed line: the spin-propagator in the double dot $\hat{D}(\omega)$, see (11), (12).

The propagators of the field in the double dot $\hat{D}(i\omega_n)$ and in the electronic reservoir $\hat{G}(i\omega_n, k)$ are given by

$$\hat{D}(i\omega_n) = \frac{1}{(i\omega_n)} \left(\hat{1}_2 \otimes \hat{1}_2\right), \tag{11}$$

$$\hat{G}(i\omega_n, k) = \frac{1}{i\omega_n - \xi_k} \times \begin{bmatrix} \cos^2\eta_k & \cos\eta_k \sin\eta_k \\ \cos\eta_k \sin\eta_k & \sin^2\eta_k \end{bmatrix} \otimes \hat{1}_2. \tag{12}$$

One can see that in comparison to the pure $SU(2) \otimes SU(2)$ Kondo effect as predicted for sequentially coupled dots, the presence of mixing between the reservoirs results in a nontrivial structure of the fermion propagator $\hat{G}(i\omega_n, k)$ in orbital space. After integration in the infinitesimal energy shell between $\Lambda - \delta\Lambda$ and Λ, Λ being the high energy cutoff, the correction to the Hamiltonian can be written as

$$\begin{aligned} \delta\hat{H}_K = {} & \pi\nu_F \left(\delta\Lambda/\Lambda\right) J_{\mu\nu} J_{\mu'\nu'} \hat{\Phi}^\dagger \times \\ & \left[\left(\hat{\tau}^\mu \otimes \hat{\tau}^\nu\right)\left(\hat{\tau}^{\mu'} \otimes \hat{\tau}^{\nu'}\right) - \left(\hat{\tau}^{\mu'} \otimes \hat{\tau}^{\nu'}\right)\left(\hat{\tau}^\mu \otimes \hat{\tau}^\nu\right)\right] \hat{\Phi} \times \\ & \hat{\Psi}^\dagger \left[\left(\hat{\sigma}^\mu \otimes \hat{\sigma}^\nu\right) \hat{P} \left(\hat{\sigma}^{\mu'} \otimes \hat{\sigma}^{\nu'}\right) - \left(\hat{\sigma}^{\mu'} \otimes \hat{\sigma}^{\nu'}\right) \hat{P} \left(\hat{\sigma}^\mu \otimes \hat{\sigma}^\nu\right)\right] \hat{\Psi}. \end{aligned} \tag{13}$$

Here ν_F denotes the density of states at the Fermi level,

$$\hat{P} = \left(b_0 \hat{1}_2 + \sum_{p=1}^{3} b_p \hat{\sigma}_p \right) \otimes \hat{1}_2,$$

$b_0 = 1/2$, and the values of other constants b_p are given by the following averages over the wave vector k

$$b_1 = \langle \cos \eta_k \sin \eta_k \rangle, \tag{14}$$

$$b_2 = 0, \text{ for } \eta_k^s = \eta_k^d, \tag{15}$$

$$b_3 = \frac{1}{2} \langle \cos^2 \eta_k - \sin^2 \eta_k \rangle. \tag{16}$$

Due to the nontrivial structure of the fermion propagator new interactions are generated in course of the renormalization group (RG) transformation. The new interactions have the structure

$$J_{\mu\lambda\nu} \hat{\Phi}^\dagger \left(\hat{\tau}^\mu \otimes \hat{\tau}^\nu \right) \hat{\Phi} \cdot \hat{\Psi}^\dagger \left(\hat{\sigma}^\lambda \otimes \hat{\sigma}^\nu \right) \hat{\Psi},$$

where all the indices μ, λ and ν change independently.

We consider the case where the tunnel couplings to the two dots are symmetric, that is $b_3 = 0$. The mixing between the two reservoirs is now determined by the value of the parameter b_1. The case $b_1 = 0$ corresponds to the case of two strictly separated reservoirs, where the $SU(4)$ Kondo effect is expected, whereas the maximal value $b_1 = b_0 = 1/2$ corresponds to a single common reservoir for both quantum dots. In the latter case only the spin $SU(2)$ Kondo effect is possible. The chosen form of the operator $\hat{P}$ with $b_1 \neq 0$ distinguishes the coupling constants with $\mu, \lambda = \overline{0,1}$. It turns out that the only coupling constants with $\mu \neq \lambda$ that are generated by the RG-transformation are $J_{10\nu}$ and $J_{01\nu}$. The constants with $\mu = \lambda = \overline{2,3}$ have the same RG-flow, we further denote them as $J_{\perp\nu}$. Without loss of generality we take the direction of the Zeeman magnetic field along the z-axes. We use the approximation that the Zeeman field freezes out the spin fluctuations as soon as the running value of Zeeman energy equals the high energy cutoff Λ. The condition for the running Zeeman energy $h(l_h) = h_0 e^{l_h} = \Lambda$ determines the logarithmic energy scale l_h. For the logarithmic energy scale $l < l_h$ the influence of the Zeeman field is neglected, all the spin components being equivalent. For $l > l_h$ the structure of the RG-equation changes abruptly, the couplings with the spin-index $\nu = 1, 2$ stop to flow.

In what follows we absorb the density of states ν_F into the definition of coupling constants $\pi \nu_F J_{\mu\lambda\nu} \mapsto J_{\mu\lambda\nu}$. For $l < l_h$, the RG-equations for the coupling constants can be written as

$$\frac{d}{dl}Q = Q^2 + R^2 + \bar{J}^2, \tag{17}$$

$$\frac{d}{dl}R = 2QR, \tag{18}$$

$$\frac{d}{dl}\bar{J} = \frac{3}{2}Q\bar{J} + K\bar{J}, \tag{19}$$

$$\frac{d}{dl}K = \bar{J}^2. \tag{20}$$

Here the following combinations of coupling constants are introduced:

$$Q = 2(b_0 J_{11\nu} + b_1 J_{10\nu}), \tag{21}$$

$$R = 2(b_1 J_{11\nu} + b_0 J_{10\nu}), \tag{22}$$

$$\bar{J} = 2\sqrt{b_0^2 - b_1^2}\, J_{\perp\nu}, \tag{23}$$

$$K = b_0 J_{110} + b_1 J_{100} \tag{24}$$

with $\nu = \overline{0,3}$. Numerical solution of the RG-equations (17)–(20) allows to determine approximately the Kondo temperature as a function of b_1. The solution is shown in the inset in Fig. 2. One can see that without the external Zeeman field, or for Zeeman energy less than the Kondo temperature $T_K^{SU(4)}$, the Kondo temperature diminishes only slightly between the SU(4)-symmetric point $b_1 = 0$ and the SU(2) symmetric point $b_1 = 0.5$. Therefore, the transition between the $SU(4)$ and $SU(2)$ Kondo effect can hardly be seen in the change of the Kondo temperature without the external Zeeman field [10].

For $l > l_h$ the RG equations have a form

$$\frac{d}{dl}\mathcal{K} = \mathcal{J}^2, \tag{25}$$

$$\frac{d}{dl}\mathcal{J} = \mathcal{K}\mathcal{J} \tag{26}$$

with

$$\mathcal{J} = \sqrt{b_0^2 - b_1^2}(J_{\mu\mu 0} + J_{\mu\mu 3}),\ \mu = \overline{2,3}, \tag{27}$$

$$\mathcal{K} = b_0(J_{110} + J_{113}) + b_1(J_{100} + J_{103}). \tag{28}$$

Eqs. (25), (26) are to be solved with the initial conditions given by the solution of (17) – (20) at $l = l_h$: $\mathcal{J}(0) = \bar{J}(l_h)$, $\mathcal{K}(0) = K(l_h) + Q(l_h)/2$.

Eqs. (25), (26) also describe the suppression of the Kondo temperature in a quantum dot coupled to ferromagnetic leads [14]. Analytical solution of (25), (26) results in the following dependence of the Kondo temperature on the Zeeman field

$$T_K(h) = h\left[\frac{\mathcal{J}(0)}{\mathcal{K}(0)+\sqrt{\mathcal{K}^2(0)-\mathcal{J}^2(0)}}\right]^{\frac{1}{\sqrt{\mathcal{K}^2(0)-\mathcal{J}^2(0)}}}. \qquad (29)$$

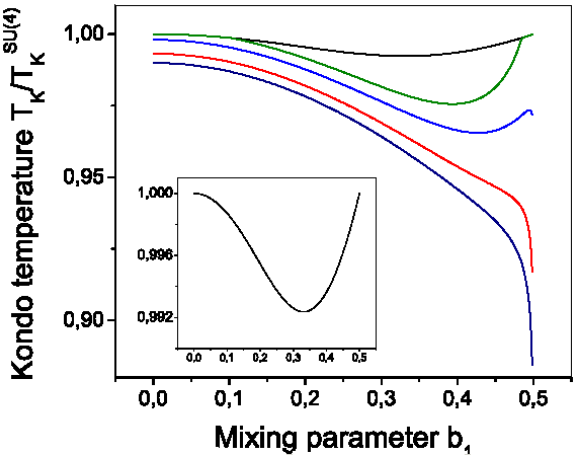

Figure 2: Kondo temperature as a function of mixing b_1 for different Zeeman fields h. Magnetic field increases from the highest to the lowest curve. From the highest to the lowest curve: $h/T_K^{SU(4)} = 1.0; 1.02; 1.06; 1.14; 1.29$. Inset: the dependence $T_k(b_1)$ at zero Zeeman field. The curves illustrate characteristic $T_K(b_1)$ dependencies.

The dependence of the Kondo temperature on the parameter b_1 at different values of Zeeman magnetic field h is shown in Fig. 2. Rising the Zeeman field, the dependence $T_K(b_1)$ changes from the nonmonotonous one to the monotonously falling. Interesting enough is the nonmonotonus dependence of Kondo temperature on the mixing parameter b_1 at relatively small Zeeman fields. The dip in the $T_K(b_1)$ dependence at intermediate values of b_1 can be explained in term of channel blocking, a common phenomenon in transport through quantum dots [15]. Namely, the two projections of the pseudospin correspond to the two transport channels through the double quantum dot. The wave functions in the channels are given by symmetric

and antisymmetric combinations of the wave functions of each dot. For the sake of brevity we further denote those channels the symmetric one and the antisymmetric one respectively. Increasing b_1, one channel (the antisymmetric one) becomes progressively decoupled from the leads. Close to the maximal possible value $b_1 = 0.5$ that channel is almost decoupled, the Kondo correlations occur only in the strongly coupled symmetric channel leading to the spin Kondo effect. Yet there is a small probability that the antisymmetric channel is occupied by an electron.

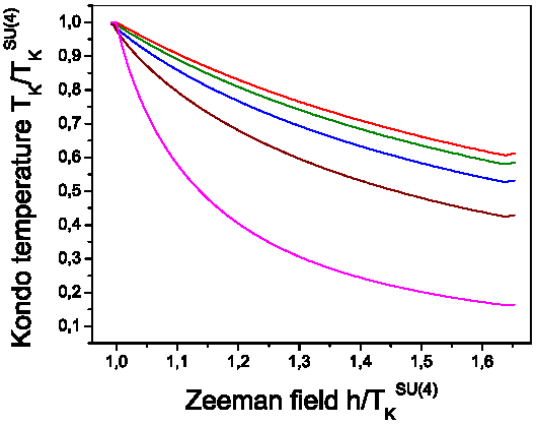

Figure 3: Kondo temperature versus Zeeman magnetic field at different values of mixing b_1. From the highest to the lowest curve $b_1 = 0.1; 0.2; 0.3; 0.4; 0.49$.

Such an event has a huge destructive influence on the Kondo effect. Not only is the spin Kondo effect suppressed in the weakly coupled channel because of a very low Kondo temperature, the Kondo effect in the strongly coupled channel is also blocked because the Coulomb blockade prevents the occupation of the symmetric state as long as the antisymmetric one is occupied. Weak coupling of the antisymmetric channel to the leads results in the long life time of an electron in that state, although the probability to occupy it by tunneling from a lead is small. The competition of a long lifetime and a low occupation probability of the blocking channel leads finally to a nonmonotonous dependence of the Kondo temperature on the mixing parameter b_1.

The dependence of the Kondo temperature on Zeeman magnetic field h for different values of the mixing parameter b_1 is shown in Fig. 3. The sup-

pression of the Kondo temperature with Zeeman field and with the mixing b_1 illustrates our findings (29).

4 Conductance of the double quantum dot device

To calculate the current through the double-dot device in presence of the applied voltage, we start with the generalization of the Kondo Hamiltonian (10) taking into account the couplings that are generated in course of RG-transformation. The current operator is defined as an electric charge flow out of the source lead

$$\begin{aligned}\hat{\jmath} &= -e\frac{\partial}{\partial t}\left(\sum_k \hat{\Psi}_k^{s\dagger}\hat{\Psi}_k^s\right)\\ &= -ie\sum_{\lambda,\mu,\nu=0}^{3}\sum_{p,p'} J_{\lambda\mu\nu}^{pp'}\hat{\Phi}^\dagger\left(\hat{\tau}^\mu\otimes\hat{\tau}^\nu\right)\hat{\Phi}\times\\ &\left[\hat{\Psi}_p^\dagger\left(\hat{\sigma}^\lambda\otimes\hat{\sigma}^\nu\right)\hat{\Psi}_{p'}, \sum_k \hat{\Psi}_k^{s\dagger}\hat{\Psi}_k^s\right]_-. \end{aligned} \tag{30}$$

Using the relation (9) between the operators $\hat{\Psi}_k$ and $\hat{\Psi}_k^s$, and evaluating the commutator in (30), we can represent the current operator in the form

$$\hat{\jmath} = \hat{\jmath}_{\rm sd} - \hat{\jmath}_{\rm ds}, \tag{31}$$

where

$$\begin{aligned}\hat{\jmath}_{\rm sd} = -ie\sum_{\lambda\mu\nu}\sum_{kk'} J_{\lambda\mu\nu}^{kk'}\frac{t_k^d t_{k'}^s}{t_k t_{k'}}\hat{\Psi}_k^{d\dagger}\left(\hat{\sigma}^\lambda\otimes\hat{\sigma}^\nu\right)\hat{\Psi}_{k'}^s\times\\ \hat{\Phi}^\dagger\left(\hat{\tau}^\mu\otimes\hat{\tau}^\nu\right)\hat{\Phi}.\end{aligned} \tag{32}$$

We are going to calculate the current to the lowest nonzero order in the renormalized Kondo coupling constants. To proceed with further calculation we note that it is only the field $\hat{\Psi}_k$ defined by (9) that acquires the renormalization by Kondo interactions. Therefore, it is convenient to express the fields $\hat{\Psi}_k^{s,d}$ through the field $\hat{\Psi}_k$ and its orthogonal

$$\hat{\Xi}_{\mathbf{k}} = \frac{t_k^d}{t_k}\hat{\Psi}_k^s - \frac{t_k^s}{t_k}\hat{\Psi}_k^d \tag{33}$$

In terms of the fields $\hat{\Psi}_k$ and $\hat{\Xi}_k$ the total current is given by

$$\hat{j} = \hat{j}_{\rm sd} - \hat{j}_{\rm ds} = -ie \sum_{\lambda\mu\nu} J_{\lambda\mu\nu} \hat{\Phi}^\dagger \left(\hat{\tau}^\mu \otimes \hat{\tau}^\nu\right) \hat{\Phi} \times$$
$$\sum_{kk'} \frac{t_k^{\rm s} t_{k'}^{\rm d}}{t_k t_{k'}} \left[\hat{\Psi}_k^\dagger \left(\hat{\sigma}^\lambda \otimes \hat{\sigma}^\nu\right) \hat{\Xi}_{k'} - \hat{\Xi}_k^\dagger \left(\hat{\sigma}^\lambda \otimes \hat{\sigma}^\nu\right) \hat{\Psi}_{k'}\right]. \tag{34}$$

The current at finite transport voltage is calculated using Keldysh formalism. The unperturbed Green's functions in the source and in the drain read

$$\hat{G}_{\rm s,d}(\epsilon, k) = \begin{pmatrix} G^R_{\rm s,d}(\epsilon,k) & G^K_{\rm s,d}(\epsilon,k) \\ 0 & G^A_{\rm s,d}(\epsilon,k) \end{pmatrix}, \tag{35}$$

where

$$G^{R/A}_{\rm s,d}(\epsilon,k) = \frac{1}{\epsilon - \xi_k^{\rm s,d} \pm io} \hat{\Theta}_{\rm s,d}(k) \tag{36}$$
$$G^K_{\rm s,d}(\epsilon,k) = \tanh\left(\frac{\epsilon - \mu_{\rm s,d}}{2T}\right) \left(G^R_{\rm s,d}(\epsilon,k) - G^A_{\rm s,d}(\epsilon,k)\right), \tag{37}$$

where $\hat{\Theta}_{\rm s,d}(k)$ is the matrix characterizing the tunneling angles for each mode

$$\hat{\Theta}_{\rm s,d}(k) = \begin{pmatrix} \cos^2\eta_k^{\rm s,d} & \cos\eta_k^{\rm s,d}\sin\eta_k^{\rm s,d} \\ \cos\eta_k^{\rm s,d}\sin\eta_k^{\rm s,d} & \sin^2\eta_k^{\rm s,d} \end{pmatrix} \otimes \hat{1}_2. \tag{38}$$

Using relations (9), (33), we obtain the following set of unperturbed Green's functions

$$\mathcal{G}_0 = -i\left\langle \hat{\Psi}\hat{\Psi}^\dagger \right\rangle_0 = \frac{(t^s)^2}{t^2} G_s + \frac{(t^d)^2}{t^2} G_d, \tag{39}$$
$$\mathcal{F}_0 = -i\left\langle \hat{\Xi}\hat{\Psi}^\dagger \right\rangle_0 = -i\left\langle \hat{\Psi}\hat{\Xi}^\dagger \right\rangle_0$$
$$= \frac{t^s t^d}{t^2}\left(G_s - G_d\right), \tag{40}$$
$$g_0 = -i\left\langle \hat{\Xi}\hat{\Xi}^\dagger \right\rangle_0 = \frac{(t^d)^2}{t^2} G_s + \frac{(t^s)^2}{t^2} G_d. \tag{41}$$

Here we suppressed the spatial and temporal arguments of the Green's functions as well as their indices in Keldysh space. Now we calculate the Kondo correction to the current through the double dot using the diagrammatic

expansion based on the Green's functions (39) – (41). Note that according to the structure of the Kondo interaction term in (10) it is only the Green function (39) that acquires corrections from the Kondo interaction. The diagram elements are represented in Fig. 4. The lowest order nonzero correction to the current is given by the diagram in Fig. 5.

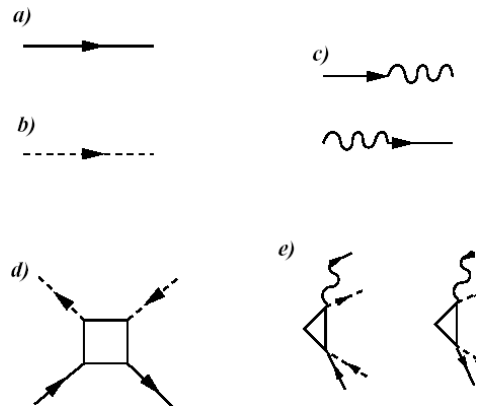

Figure 4: Elements of the diagrams: a) $\mathcal{G}_0$; b) semifermion Green's function; c) $\mathcal{F}_0$; d) Kondo interaction vertex; e) vertices for the current operator.

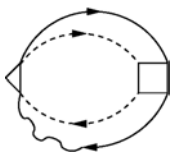

Figure 5: Diagram for the lowest order nonzero contribution to the current through the double quantum dot.

Further calculation is performed for symmetric couplings to the source and to the drain, that is for $t^s_{ik} = t^d_{ik}$. In that case the tunneling angles of each mode in the source and in the drain leads are equal, $\eta^s_k = \eta^d_k$. Furthermore, as it has already been done in calculations of the Kondo temperature (see Section 3), we neglect a possible dependence of the total tunneling to the double quantum dot on the absolute value of the wave vector $|k|$. Then, as follows from the definition (40), the components of the Green's function

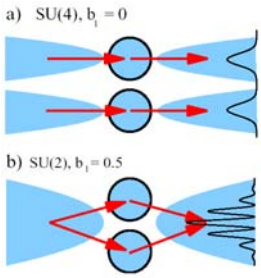

Figure 6: a) Scheme of conducting channels in the $SU(4)$ Kondo effect. There are two conductance channels with correlated transport but without interference. The total current is given by the sum of currents through each channel. b) Scheme of conducting channels in the spin $SU(2)$ Kondo effect in double quantum dot. The double slit geometry is realized. There is a single channel that is splitted between the two quantum dots. The total current is given by interference of the two partial waves in the central maximum.

$\mathcal{F}^{R/A}$ vanish, and the only nonzero component of the function $\mathcal{F}$ reads

$$\mathcal{F}^K(\epsilon,k) = (-2\pi i)\frac{t^s t^d}{t^2}\left\{\tanh\left(\frac{\epsilon-\mu_s}{2T}\right)\right.$$
$$\left.-\tanh\left(\frac{\epsilon-\mu_d}{2T}\right)\right\}\delta(\epsilon-\xi_k). \tag{42}$$

Performing the evaluation of the diagram in Fig. 5, we obtain the expression for total current through the double quantum dot in the form

$$j(V) = 40\pi e^2 V\nu_0^2\frac{\left(t^s t^d\right)^2}{t^4}\sum_{\lambda,\mu,\nu}J^2_{\lambda\mu\nu}\left(\frac{1}{2}+2b_1^2\right). \tag{43}$$

Here ν_0 denoted the one particle density of states in the source and drain leads. Let us comment on the origin of different factors in (43). The factor $\sum_{\lambda\mu\nu}J^2_{\lambda\mu\nu}$, where the sum runs over the whole set of the Kondo coupling constants generated by the RG transformation, reflects the influence of the spin and orbital Kondo correlations on the current through the double dot. In contrast, the term $\frac{1}{2}+2b_1^2$ describes the single particle interference effects by transport through the double dot device. Namely, in the case $b_1 = 0$, when each dot has its own reservoir of modes in the source and in the drain lead, the current through the device is obtained as a sum of the currents

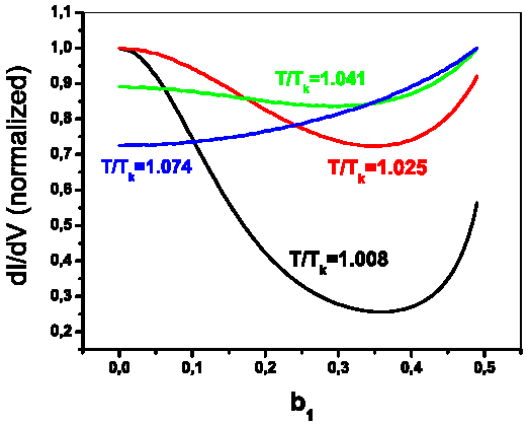

Figure 7: Differential conductance of the double quantum dot vs the mixing parameter b_1 at different temperatures. The nonmonotonous behavior close to the Kondo temperature is dominated by correlation effects, while the interference effects lead to the monotonous increase of the differential conductance with b_1 at higher temperatures.

through the dot 1 and through the dot 2 (see Fig. 6a). In the other limit case $b_1 = 1/2$, there is a common reservoir for both dots. Then a typical geometry of a double-slit experiment is realized. Due to the interference effect, the current in the interference maximum is doubled with respect to its classical value. Indeed, the value of the factor $\frac{1}{2} + 2b_1^2$ is twice as much for $b_1 = 1/2$ as for $b_1 = 0$ (see Fig. 6b). At the intermediate values of b_1 the single particle coherence is partially suppressed.

The correlation factor dominates the dependence of the differential conductance at temperatures close to the Kondo temperature, whereas the single particle interference determines the behavior of conductance at higher temperatures further away from T_K. These findings are illustrated in Fig. 7.

According to the behavior of the conductance as a function of the mixing parameter b_1, the low-temperature and the high-temperature regimes can be identified that are dominated by the many particle corelations or by the single particle interference respectively.

Suppressing the Kondo correlations in the spin sector by a Zeeman magnetic field, one extends the regime, where the single particle interference dominates the behavior of conductance. At finite Zeeman magnetic field, the regimes of high and low field can be identified according to the qualitative behavior of the conductance, as shown in Fig. 8. In the high tempera-

ture regime, the conductance increases monotonously with b_1 at all Zeeman fields. Increasing the Zeeman field affects only the conductance at small values of b_1 suppressing it. At b_1 close to 0.5 and Zeemann field, both spin and pseudospin Kondo correlations are suppressed, and the conductance is determined by the single particle interference factor only.

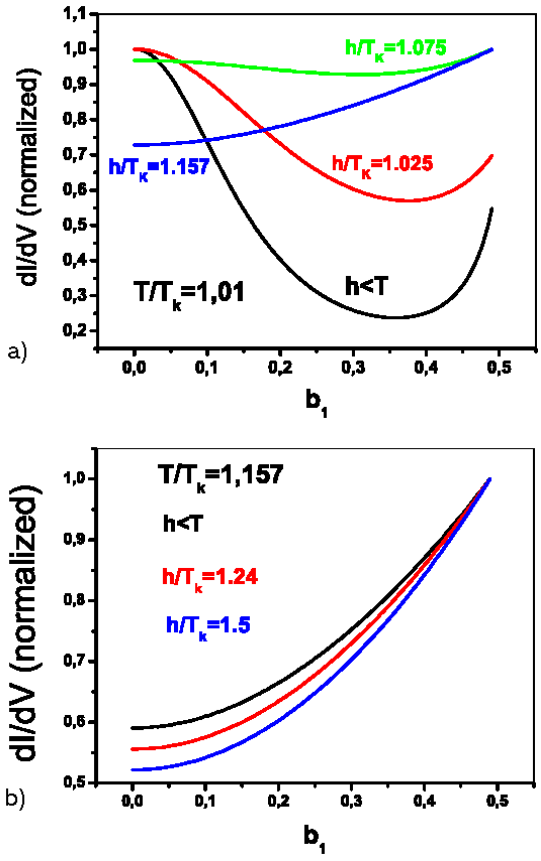

Figure 8: Differential conductance of the double quantum dot as a function of the mixing parameter b_1 at different Zeeman fields. a) Low temperature regime: The change from nonmonotonous behavior to the monotonous increase is due to the suppression of Kondo correlations by Zeemann field. b) High temperature regime: The behavior of conductance is dominated by the one-particle interference.

5 Conclusion

In this work we considered the transition between the SU(4) and SU(2) Kondo effects in a double dot system embedded in a parallel circuit with attached leads. The transition is induced by the transfer of electrons between that dots through the leads, which violates the conservation of the pseudospin. Despite having the same Kondo temperature, the SU(4) and spin SU(2) Kondo effects can be distinguished by the sensitivity to the in plane Zeeman magnetic field. We derived the dependence of the Kondo temperature on Zeeman magnetic field (29) that allows direct comparison with experiments. Being the basic energy scale, the Kondo temperature determines all other experimentally observable properties related to the Kondo effect. In particular, the behavior of the differential conductance through the double quantum dot as a function of the mixing parameter b_1 is determined by the interplay of two factors, the suppression of the pseudospin Kondo correlations with b_1 and the increase of the single particle coherence. Domination of the correlation factor leads to the dependence of conductance that is similar to the dependence of the Kondo temperature on b_1, while the dominance of the interference factor leads to the monotonous increase of the differential conductance with the mixing parameter b_1.

One can propose several ways to change the mixing between the reservoirs in experiment. Starting from the case of fully mixed reservoirs $b_1 = 0.5$ the separation can be achieved by diminishing the single particle coherence length. As soon as the coherence length is smaller than the separation between the two dots, the coherent propagation of electrons between the two dot through the source or through the drain leads becomes suppressed, and each dot is coupled to its own subset of modes, which corresponds to the case $b_1 = 0$ (see Fig. 6a).

Therefore, the calculated dependence of the Kondo temperature and of the differential conductance on Zeeman magnetic field and on the mixing parameter can be seen in the measurements of the conductance through the double quantum dot device. The obtained results can also be relevant to the experiments on Kondo effect in carbon nanotubes [10].

A.C. and F.H. thank D. Pfannkuche and M. Trushin for valuable comments. Support from Deutsche Forschungsgemeinschaft through Sonderforschungsbereiche SFB 508 (F.H., V.K.) and SFB 668 (A.C.) is gratefully acknowledged.

References

[1] D. Goldhaber-Gordon, H. Shtrikman, D. Mahalu, D. Abusch-Magder, U. Meirav, and M.A. Kastner, Nature **391**, 156 (1998); S.M. Cronenwett, T.H. Oosterkamp, and L.P. Kouwenhoven, Science **281**, 540 (1998);

[2] S. Sasaki, S. De Franceschi, J.M. Elzerman, W.G. van der Wiel, M. Eto, S. Tarucha, and L.P. Kouwenhoven, Nature **405**, 764 (2000); M. Eto and Y.V. Nazarov, Phys. Rev. Lett. **85**, 1306 (2000); M. Pustilnik and L.I. Glazman, Phys. Rev. Lett. **85**, 2993-2996 (2000); B. Dong and X.L. Lei, Phys. Rev. B **66**, 113310 (2002).

[3] A.W. Holleitner, R.H. Blick, A.K. Huettel, K. Eberl, and J.P. Kotthaus, Science **297**, 70 (2002); A.W. Holleitner, A. Chudnovskiy, D. Pfannkuche, K. Eberl, and R.H. Blick Phys. Rev. B 70, 075204 (2004).

[4] U. Wilhelm, J. Schmid, J. Weis, and K. von Klitzing, Physica E **9**, 625 (2001); Physica E **14**, 385 (2002).

[5] L. Borda, G. Zarand, W. Hofstetter, B.I. Halperin, and J. von Delft, Phys. Rev. Lett. **90**, 026602 (2003).

[6] G. Zarand, Phys. Rev. B **52**, 13459 (1995).

[7] K. Le Hur and P. Simon, Phys. Rev. B **67**, 201308(R) (2003); K. Le Hur, P. Simon, and L. Borda, Phys. Rev. B **69**, 045326 (2004).

[8] P. Jarillo-Herrero, Jing Kong, H.S.J. van der Zant, C. Dekker, L.P. Kouwenhoven, and S. De Franceschi, Nature **404**, 484 (2005).

[9] R. Lopez, D. Sanchez, M. Lee, Mahn-Soo Choi, P. Simon, and K. Le Hur, Phys. Rev. B **71**, 115312 (2005). This work discusses the crossover between $SU(4)$ and $SU(2)$ Kondo effect induced by an orbital effect of external magnetic field. In this case, two mutually orthogonal linear combinations of the wave functions of source and drain leads provide with the two completely separated electronic reservoirs, the pseudospin in reservoirs thus being well-defined.

[10] M-S. Choi, R. Lopez, R. Aguado, Phys. Rev. Lett. **95**, 067204 (2005).

[11] Similar SU(4) to SU(2) crossover has been considered recently for the half-filling (two electrons in the double quantum dot) in C.A. Büsser and C.B. Martins, Phys. Rev. B **75**, 045406 (2007).

[12] A.L. Chudnovskiy, Europhys. Lett. **71**, 672 (2005).

[13] L.I. Glazman and M.E. Raikh, JETP Lett. **47**, 452 (1988).

[14] J. Martinek, Y. Utsumi, H. Imamura, J. Barnas, S. Maekawa, J. König, and G. Schön, Phys. Rev. Lett. **91**, 127203 (2003).

[15] D. Jacob, B. Wunsch, and D. Pfannkuche, Phys. Rev. B **70**, 081314 (2004).